World Academy of Science, Engineering and Technology
International Journal of Civil and Environmental Engineering
Vol:7, No:12, 2013

Design of Rigid L- Shaped Retaining Walls

A. Rouili

***Abstract*—**Cantilever L-shaped walls are known to be relatively economical as retaining solution. The design starts by proportioning the wall dimensions for which the stability is checked for. A ratio between the lengths of the base and the stem, falling between 0.5 to 0.7 ensure in most case the stability requirements, however, the displacement pattern of the wall in terms of rotations and translations, and the lateral pressure profile, do not have the same figure for all wall's proportioning, as it is usually assumed. In the present work the results of a numerical analysis are presented, different wall geometries were considered. The results show that the proportioning governs the equilibrium between the instantaneous rotation and the translation of the wall-toe, also, the lateral pressure estimation based on the average value between the at-rest and the active pressure, recommended by most design standards, is found to be not applicable for all walls.

***Keywords*—**Cantilever wall, proportioning, numerical analysis.

I. Introduction

RIGID cantilever L - shaped retaining walls are considered as complex type of geotechnical structures, particularized by the fact that they are not only supported by the soil, as is the case with foundations, but also loaded by the soil. Actual design methodology does not take into account the real geometry of the wall and the acting lateral pressure magnitude and distribution. Most of the well known codes of practices assume a simple hydrostatique stress distribution, acting on 'the virtual' wall, based on the Coulomb's and Rankine's theories. The geometry (shape and dimensions) is a key issue in investigating retaining structures. Previous researches suggest different values of the ratio of the wall height to base. An average value of 0.5 was suggested by Powerie and Chandler [1], and suggested later as optimum by Daly and Powerie [2]. It is obvious that there is no clear guidance on the value of this ratio. It is suggested in the followings, to investigate the effect of the 'dimensions' parameters on the overall behavior of the particular L-shaped retaining wall.

In the present investigation the effect of the geometry (designated by *WH* and the ratio *B/H*) on the behavior of the L-shaped rigid retaining wall is investigated with a numerical model, developed and validated with respect to the geometry, dimensions, boundary conditions and the loading conditions of a reference system presented in Fig. 1. This system was investigated by previous researchers in a centrifuge experiment conducted on a reduced scale prototype [3].

A. Rouili is with the University of Tebessa, Faculty of Sciences and Technology, Tebessa, Algeria (e-mail: arouili@hotmail.com).

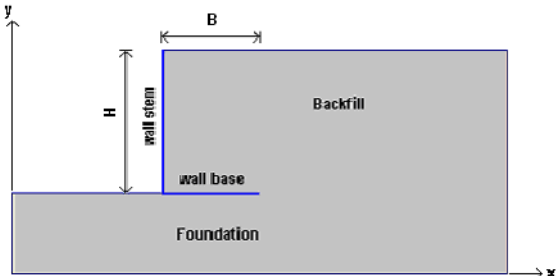

Fig. 1 Reference system

II. Geometry of the Wall

In order to investigate the effect of the height of the wall and the horizontal length of the base, 3 L-shaped walls were considered: a 2m height wall (designated by *WH2*), a 5m height wall (*WH5*) and a 9m height wall (*WH9*). The walls considered remain very stiff. To account for the effect of the base on the lateral pressure distribution, the ratio *B/H* was introduced as variable parameter, where *H* is the height of the stem of the wall and *B* is the corresponding horizontal base length: 4 ratios were investigated in the present study, 0.3, 0.5, 0.8 and 1.0 to account for the lower bound and the upper bound behaviors, and includes the actual design practice, recommended values falling between 0.5 and 0.8 [4].

The present approach allowed to investigate the direct effect of the parameters *H* and *B/H* on the displacement pattern and the lateral pressure acting on the L–shaped retaining wall. The values of *H* considered were assumed to represent the behavior of distinctive wall dimensions including the height of the wall considered in the development of the numerical model (H=9m). The combination of the (*H*) and (*B/H*) parameters yields to the numerical analysis of 12 different L-shaped retaining walls. The designation adopted for the different parametric walls is presented in the Table I, were for example the wall designated by *WH2BH03* stands for a 2 meter height L-shaped wall with a ratio of its height over the length of its base *(H/B*) equal to 0.3 (*BH03*).

TABLE I
Designation of the Parametric Walls

	B/H			
***H* (m)**	**0.3**	**0.5**	**0.8**	**1.0**
2	*WH2BH03*	*WH2BH05*	*WH2BH08*	*WH2BH1*
5	*WH5BH03*	*WH5BH05*	*WH5BH08*	*WH5BH1*
9	*WH9BH03*	*WH9BH05*	*WH9BH08*	*WH9BH1*

III. Soil and Walls Modeling

The numerical analysis was carried out in plane strain, the entire model extends 28m horizontally and 14m vertically, to account for the centrifuge dimensions box converted to the

prototype scale. The retaining walls are defined through an L-Shaped beam (with a rigid slab footing) representing the prototype dimensions of the centrifuge model. Conditions of plane strain were assumed throughout. Fig. 2 shows a typical finite element model with the displacement boundary conditions. The retaining wall was modeled by beam elements with a Young's modulus (reinforced concrete) assumed with $E_b = 3 \cdot 10^4$ MN/m2. The soil has been modeled using the hardening soil model, considered in drained conditions [5]. The soil modeling parameters are presented in Table II.

TABLE II
MODELING PARAMETERS OF THE SOIL

$E_{oed\ ref}$ [MN/m^2]	$E_{50\ ref}$ [MN/m^2]	$E_{ur\ ref}$ [MN/m^2]	m	Φ [°]	c	Ψ [°]
25	25	100	0.65	35	0	2.5

The numerical modeling concept used for the validation of the numerical model developed together with its possible limitations has been fully investigated by Rouili et al. [6] and [7].

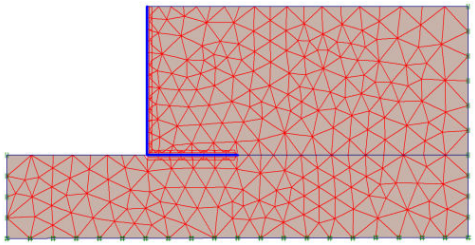

Fig. 2 Typical finite element model

IV. Numerical Calculations and Results

The calculation was carried for each wall separately; the calculation process starts from a stage of initial condition with different wall dimensions. The calculation progresses until the prescribed ultimate state is fully reached. A typical post processing deformed meshes corresponding to the walls *WH5BH05 is* presented in Fig. 3.

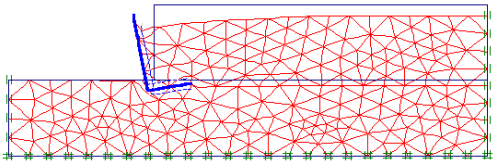

Fig. 3 Typical deformed mesh (wall *WH05BH05*)

V. Displacement of the Wall

For all the walls the bending deflection are negligible and the measured horizontal and vertical displacements reported concerns the rigid body movements. As illustrated in Fig. 4, δ_{ht} represents is the horizontal movement of the top of the wall (displacement of the point A_n); δ_{hb} is the horizontal movement of the bottom of the wall (horizontal displacements of the points B_n and C_n); δ_v is the vertical movement of the wall (nodal vertical displacement of the points A_n and B_n).

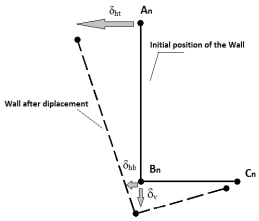

Fig. 4 Displacement Pattern of the Wall

Figs. 5-8 show the computed displacement of the nodal point B_n plotted against the multiplier, corresponding respectively to the walls having the ratio B/H =0.5 to B/H =*1*. As it is clear from these figures, the displacements path corresponding to B/H=0.3 plotted on Fig. 5 and the displacement path for B/H=0.5 plotted on Fig. 6 follows a curved lines which indicates the rotation effect, however, the displacement paths corresponding to B/H=0.8 plotted on Fig. 7 and the displacement path for B/H=1 plotted in Fig. 8 are closely linear which indicates the translation effect.

As far as the geometry if the L-shaped wall is concerned, it could be concluded from the present analysis that, the length of the wall base through the ratio B/H governs the equilibrium between the instantaneous rotation and the translation of the wall-toe. It was shown that for values of B/H less than 0.5 the rotational movement is dominant. However, for values of B/H over 0.8 the translation of the toe is more pronounced. The design practice of B/H laying between 0.5 and 0.8, remains reasonable as far as the equilibrium between the rotation and translation of the wall is concerned. These observations are summarized in the chart of Fig. 9.

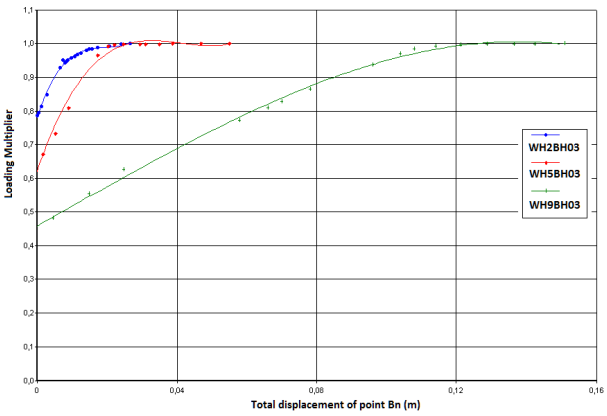

Fig. 5 Total displacements of the Point Bn (*B/H=0.3*)

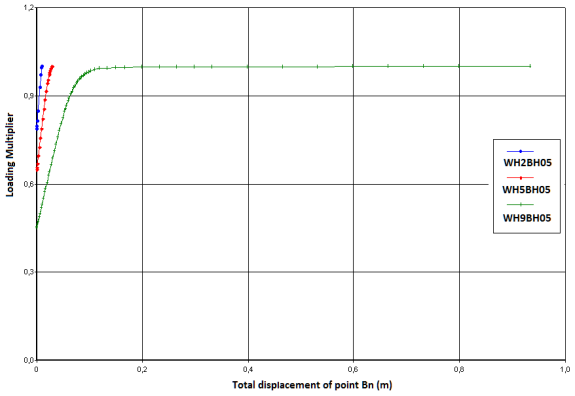

Fig. 6 Total displacements of the Point *Bn* (*B/H=0.5*)

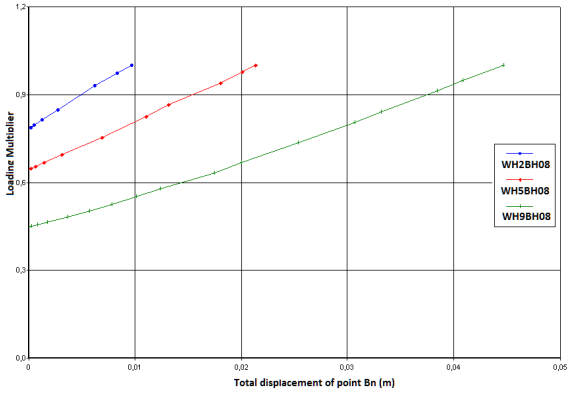

Fig. 7 Total displacements of the Point *Bn* (*B/H=0.8*)

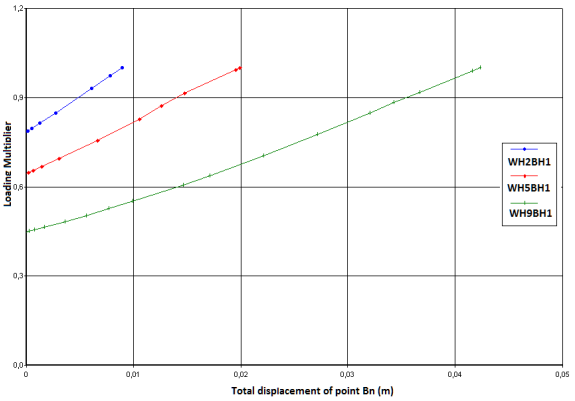

Fig. 8 Total displacements of the Point *Bn* (*B/H=1*)

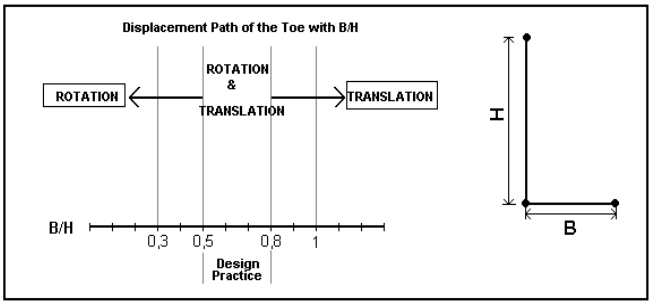

Fig. 9 Displacement chart of the L-shaped wall

VI. Lateral Pressure Acting on the Walls

Fig. 10 shows the lateral pressures profiles as a results of varying the wall-stem height (*WH*) and the ratio *B/H*. Following the increase of the ratio *B/H* for each wall, it could be noticed that the lateral pressure seem to increase accordingly, this effect could be attributed to the relative pressure applied by the weight of the backfill soil resting on the wall base. On this figures it is also plotted the repartition of the lateral pressure computed using the Rankine approach. It could be argued that as far as the distribution of the lateral pressure acting on the wall-stem is concerned, the design approach does not apply for all the L-shaped geometries investigated, especially, when the lateral pressure is estimated out of the average, between the active and the at-rest conditions. On these figures it is also evident, that in the lower third of the walls height, there is an abrupt change with deceasing values of the lateral pressure (slope), this is common to all the walls considered but at different depth noted. It could be argued that the position of the lateral pressure change depends uniquely on the height of the wall and seems not influenced by the base length.

In Fig. 11 shows the lateral pressure profiles as a result of varying the base length through the ratio *B/H* and the wall height (*WH*). From this figures it could be seen that the slopes and magnitudes of the lateral pressures acting on the different walls are nearly comparable regardless the wall-stem height.

On Fig.12 the computed lateral pressure coefficients *Kc,* corresponding to the walls *WH2, WH5* and *WH9*, for value of the ratio *B/H* falling between 0.5 and 0.8 (recommended design limits), are plotted against the variation of the coefficient of the lateral pressure. For appreciation of the results 2 bounds limits of the lateral pressure coefficient were fixed (according to the design practice), the upper limit is the presentation of the at-rest coefficient K_0, and the lower limit is the coefficient K_a corresponding to the active pressure (for δ=0), the average value i.e. 0.5 (K_a + K_0) is also plotted. From this figure it could be argued that, for all walls considered there is a unique figure, the value of *Kc* falls all above the active pressure of the soil, and seems to increase with the value of the ratio *B/H*, but remains below the average limits usually considered in design practice which implies an overestimation of the lateral pressure.

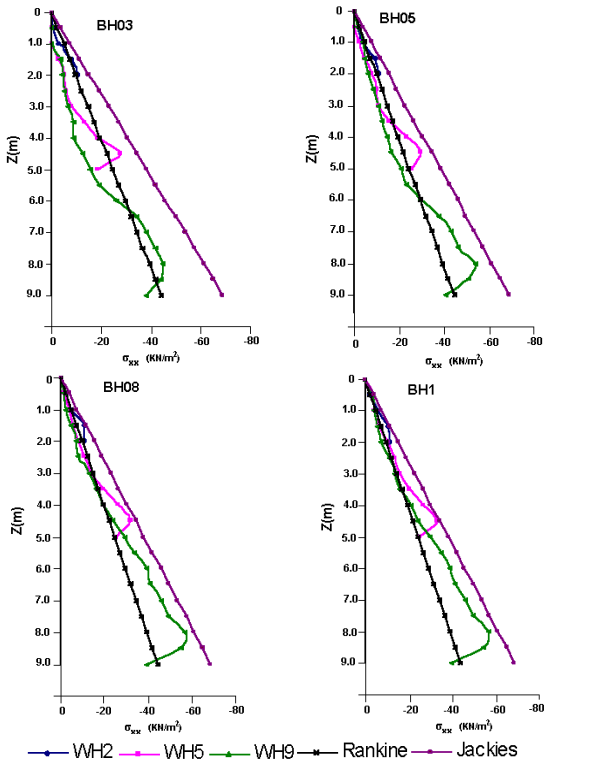

Fig. 10 Lateral pressure profile all-walls

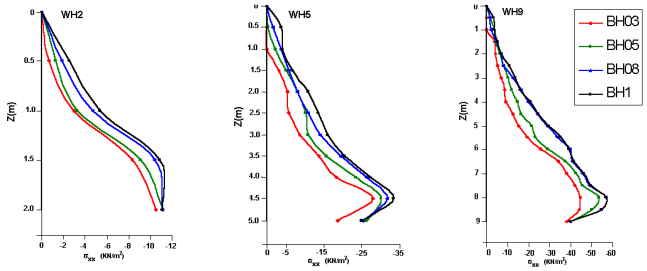

Fig. 11 Lateral pressure variation *WH*

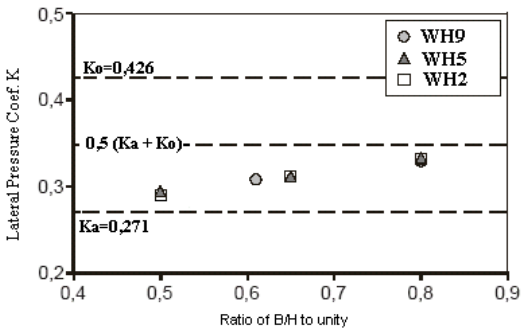

Fig. 12 Earth pressure coefficient dependent on *B/H*

VII. Conclusion

In the present work the results of a numerical analysis are presented, different wall geometries were considered. The results show that the proportioning governs the equilibrium between the instantaneous rotation and the translation of the wall-toe; also, the length of the wall base through the ratio *B/H* governs the equilibrium between the instantaneous rotation and the translation of the wall-toe. It was shown that for values of *B/H* less than 0.5 the rotational movement is dominant. However, for values of *B/H* over 0.8 the translation of the toe is more pronounced. The design practice of *B/H* lay between 0.5 and 0.8, remains reasonable as far as the equilibrium between the rotation and translation of the wall is concerned.

The lateral pressure estimation based on the average value between the at-rest and the active pressure, recommended by most design standards, is found to be not applicable for all walls. For all walls considered in the present exercise, there is a unique figure, the values of the computed lateral pressure coefficients (*Kc)* falls all above the active pressure of the soil, and seems to increase with the value of the ratio *B/H*, but remains below the average limits usually considered in design practice which implies an overestimation of the lateral pressure.

References

[1] Powrie, W. and Chandler, R. J. "*The influence of a stabilizing platform on the performance of an embedded retaining wall: a finite element study*", Geotechnique 48, No. 3, 1998, 403-409.

[2] Daly, M. and Powrie, W. "*A centrifuge and analytical study of stabilizing base retaining walls*". Transport Research Laboratory. TRL report 387, 1999.

[3] Djerbib, Y., Hird, C.C. and Touahmia, M. "*Centrifugal model tests of uniform surcharge loading on L-shaped retaining walls*." 15th International Conference on Soil Mechanics and Foundation Engineering, Istanbul, Volume 2, 2001, 1137-1140.

[4] Oliphant, J. "*The outline design of earth retaining walls*"., Ground Engineering Journal, No.9, 53-58, 1997.

[5] Schanz, T., Vermeer, *P.A. & Bonnier, P.G. The hardening soil model: Formulation and verification. In: Beyond 2000 in Computational geotechnics*– 10 Years of Plaxis. Balkema, Rotterdam, 1999.

[6] Rouili, A., Y. Djerbib and M. Touahmia. "*Numerical modeling of an L – shaped very stiff concrete retaining wall*." La Revue des Sciences et Technologie de l'Université de Constantine. B, Numéro 24. 2006, pp. 69-74.

[7] Achmus, M., and Rouili, A., "*Investigation on the earth pressure loading of L-shaped retaining walls."* "Untersuchung zur *Erdrruckbeanspruchung von Winkelstützwänden*". Ernst und Sohn-Bautechnik Journal, Germany, Volume 81, Number 12. 2004, pp. 942-948.